MODELING THE GROWTH OF BULK SINGLE CRYSTALS VIA HIGH PERFORMANCE COMPUTING

Andrew Yeckel, Yong-Il Kwon, and Jeffrey J. Derby
Department of Chemical Engineering and Materials Science &
Army High Performance Computing Research Center,
University of Minnesota, Minneapolis, MN 55455, USA

SUMMARY

We have developed new algorithms for solution of the three-dimensional, time-dependent Navier-Stokes equations that utilize massively parallel supercomputing implemented on the Connection Machine 5. Here, we apply these techniques to analyze the fluid flows that occur during the growth of the two nonlinear optical crystals – potassium dihydrogen phosphate (KDP), which is produced in a novel rapid growth system under development by the Lawrence Livermore National Laboratory Laser Division, and potassium titanyl phosphate (KTP), which is grown from a high-temperature aqueous solution.

INTRODUCTION

Solution crystal growth processes are governed by complex interactions of transport phenomena, crystal growth kinetics, and crystallography. The realistic modeling of fluid flow, mass transfer, and crystal morphology in these systems has not been possible in the past due to the extreme computational challenges posed by the truly three-dimensional, time-dependent behavior exhibited by these systems. Analysis of such systems has become feasible, however, with the advent of massively parallel supercomputers and algorithms (Tezduyar et al., 1994; Salinger et al., 1994; Xiao et al., 1995). Previously we have performed extremely large simulations needed for the study of three-dimensional flows and transport occurring in melt crystal growth systems (Derby et al., 1994; Xiao & Derby, 1995; Xiao et al., 1996). Here we present the first detailed computations ever successfully performed for analysis of three-dimensional fluid flows occurring in a solution crystal growth system.

Currently we are studying two solution crystal growth systems. One of these is the rapid growth system for KDP under development by researchers at Lawrence Livermore National Laboratory (LLNL). This aggressive program aims to grow high-quality KDP, an important nonlinear optical material, at rates greatly surpassing prior approaches (Zaitseva et al., 1995). The other system, used to grow KTP, bears some resem-

†Support for this work has been provided in part by the National Science Foundation, Lawrence Livermore National Laboratory, the University of Minnesota Supercomputer Institute, and the Army HPC Research Center under the auspices of the Department of the Army, Army Research Laboratory. The content does not necessarily reflect the position or policy of the government, and no official endorsement should be inferred.

blance to the first, and in fact the two systems share some common features with respect to hydrodynamics (Bordui et al., 1987; Bordui & Motakef, 1989).

An important aspect of increasing growth rates while maintaining high crystal quality in both systems is the use of forced convection driven by crystal and support rotation to overcome significant diffusive mass transfer limitations. The specific form of the flow field through the system is important for the control of deleterious effects, such as unwanted modification of the crystal growth habit, spurious nucleation events, and morphological instabilities of the growing crystal. (Bordui & Motakef, 1989) Calculations are presented here that demonstrate the complicated nature of three-dimensional, rotationally-driven flows in these systems.

GOVERNING EQUATIONS AND METHODS

We consider flows governed by the three-dimensional Navier–Stokes equations. The problem is solved in a rotating reference frame, which requires that terms accounting for the Coriolis force be added to Equation (Zhou, 1994). In this reference frame the crystal and support remain stationary and the walls of the tank rotate; by adopting this reference frame we avoid the need to use a moving mesh. This reference frame also is the most interesting from the physical point of view, since mixing and mass transport to the crystal are determined relative to this frame. For the analyses conducted in this study, we assume that the flow is driven only by rotation of the crystal and support and that there are no significant buoyancy effects caused by temperature or solutal variations.

The KDP problem is discretized using the Galerkin finite element method (Hughes, 1987). Hexahedral elements having 27 nodes per element are used to interpolate the velocity field with triquadratic Lagrangian polynomials. Pressure is approximated by a linear combination of discontinuous linear basis functions having 4 degrees of freedom per element. The KTP problem is discretized using the Galerkin/least-squares method (Hughes et al., 1989; Tezduyar, 1992). Tetrahedral elements having 4 nodes per element are used to interpolate velocity and pressure with linear Lagrangian polynomials. Standard procedures are applied to obtain weak-form weighted residual equations, which are solved by Newton iteration. The linear system is solved at each Newton iteration using restarted GMRES in conjunction with diagonal preconditioning.

The formulation just described is implemented on the Thinking Machines Corporation CM-5, a distributed memory, multi-processor supercomputer. Individual finite element data sets are mapped to processors, and the element-level components of the residual equations and Jacobian matrix are calculated concurrently. Matrix-vector multiplications of GMRES are conducted with element-level rather than global residual and Jacobian matrix elements. Therefore only the resulting update vectors need scattering to the global level, at which point modified Gram-Schmidt orthogonalization is performed. The orthogonal vector thereby formed is then gathered to the local level to be used in the next round of matrix-vector multiplications. Mesh partitioning is used to reduce the communications costs of these gather/scatter operations. Details of our implementation can be found in Salinger et al. (1994).

RESULTS

Figure 1 shows schematics of the two systems. The KDP system, shown in Figure 1a, consists of a solution-filled container into which hangs a support, upon which sits the crystal. The KTP system, shown in Figure 1b, is somewhat similar, except that the crystal is supported by a rod immersed in the solution. In the KDP simulations the support and crystal rotate according to the schedule in Figure 1c. In the KTP simulations the support and crystal rotate at a constant rate.

Figure 2 shows results for the KDP system, at a Reynolds number of 1267. Velocity vectors are plotted on a horizontal plane passing through the middle of the crystal. Figure 2a shows results at the time indicated on the rotation schedule in Figure 1c. At this time the system has completed eight revolutions at a constant rate in one direction. The results show that the flow direction is predominantly azimuthal. In particular, the flow near the crystal is relatively weak, exhibiting little local mixing. It is surmised that poor local mixing contributes to the formation of solute inclusions during growth.

Figure 2b shows velocity vectors on the same horizontal plane, after rotation has been temporarily halted, as indicated on the rotation schedule in Figure 1c. The figure shows that a strong radial flow has developed in the region of the crystal faces. The resulting stagnation point flow is ideal for promoting both local and global mixing of solute. Experimental results show that a rotation schedule in which rotation is temporarily halted, then reversed in direction, is necessary to prevent solute inclusions from forming in this system. The results here provide a possible explanation for the experimental observations.

To better understand and quantify mixing in this system, we have conducted numerical studies in a model system, in which the posts are absent, and the crystal and platform are approximated by axisymmetric bodies. Figure 3 shows the root-mean-square average axial (Figure 3a), and root-mean-square average radial (Figure 3b), velocities computed in the 2D axisymmetric and 3D systems. Although the 2D axisymmetric results are qualitatively similar to the 3D results, it is clear that the decay of RMS average axial and radial velocities in the 3D system occurs more rapidly during the spin-down phase of the rotation schedule. Also, the RMS average radial velocity attains a larger value during the spin-up phase. These effects indicate enhanced mixing in the 3D system, and can be attributed to the complicated geometry of the crystal support.

Figure 4 shows steady-state results for the KTP system, at a Reynolds number of 50. Velocity vectors are plotted on a vertical plane through the system axis. The figure shows that rotation of the crystal and support induces pumping of solution towards the crystal faces in the manner of a von Kármán swirling flow, thereby setting up a secondary flow of toroidal recirculations. Future simulations are planned to study transient effects in this system when subjected to the rotation schedule of Figure 1c.

REFERENCES

P. F. Bordui, J. C. Jacco, G. M. Loiacono, R. A. Stolzenberger, and J .J. Zola (1987) Growth of large single crystals of $KTiOPO_4$ (KTP) from high-temperature solution using heat pipe based furnace system. *J. Crystal Growth* **84**, 403–408.

P. F. Bordui and S. Motakef (1989) Hydrodynamic control of solution inclusion during crystal growth of KTP from high-temperature solution. *J. Crystal Growth* **96**, 405–412.

J. J. Derby, S. Brandon, A. G. Salinger, and Q. Xiao (1994) Large-scale numerical analysis of materials processing systems: High-temperature crystal growth and molten glass flows. *Comput. Methods Appl. Mech. Engrg.* **112**, 69–89.

T. J. R. Hughes (1987) *The Finite Element Method*, Prentice-Hall, Inc.

T. J. R. Hughes, L. P. Franca, and G. M. Hulbert (1989) A new finite element formulation for computational fluid dynamics: VIII. The Galerkin/least-squares method for advective-diffusive equations. *Comput. Methods Appl. Mech. Engrg.* **73**, 173–189.

A. G. Salinger, Q. Xiao, Y. Zhou, and J. J. Derby (1994) Massively parallel finite element computations of three-dimensional, time-dependent, incompressible flows in materials processing systems. *Comput. Methods Appl. Mech. Engrg.* **119**, 139–156.

T. E. Tezduyar (1992) Stabilized finite element formulations for incompressible flow computations. In J. W. Hutchinson and T. Y. Wu, editors, *Advances in Applied Mechanics*, pages 1–44. Academic Press, Inc.

T. E. Tezduyar, S. K. Aliabadi, M. Behr, and S. Mittal (1994) Massively parallel finite element simulation of compressible and incompressible flows. *Comput. Methods Appl. Mech. Engrg.* **119**, 157–177.

Q. Xiao and J. J. Derby (1995) Three-dimensional melt flows in Czochralski oxide growth: High-resolution, massively parallel, finite element computations. *J. Crystal Growth* **152**, 169–181.

Q. Xiao, S. Kuppurao, A. Yeckel, and J. J. Derby (1996) On the effects of ampoule tilting during vertical Bridgman growth: Three-dimensional computations via a massively parallel, finite element method. *J. Crystal Growth*, **167**, 292–304.

Q. Xiao, A. G. Salinger, Y. Zhou, and J. J. Derby (1995) Massively parallel finite element analysis of coupled, incompressible flows: A benchmark computation of baroclinic annulus waves. *Intern. J. Numer. Meths. Fluids* **21**, 1007–1014.

N. P. Zaitseva, L. N. Rashkovich, and S. V. Bogatyreva (1995) Stability of KH_2PO_4 and $K(H,D)_2PO_4$ solutions at fast growth rates. *J. Crystal Growth* **148**, 276–282.

Y. Zhou (1994) Finite element analysis of electrochemical machining problems, validity of electroneutrality assumption, and flow in solution crystal growth system. Ph.D. Thesis, University of Minnesota.

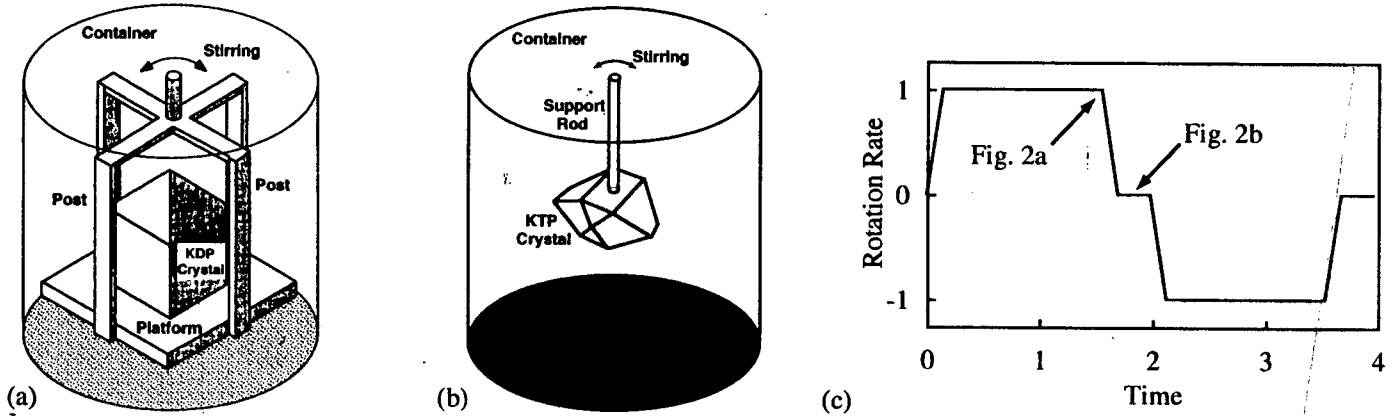

Figure 1. (a) Schematic of KDP growth system. (b) Schematic of KTP growth system. (c) Rotation schedule.

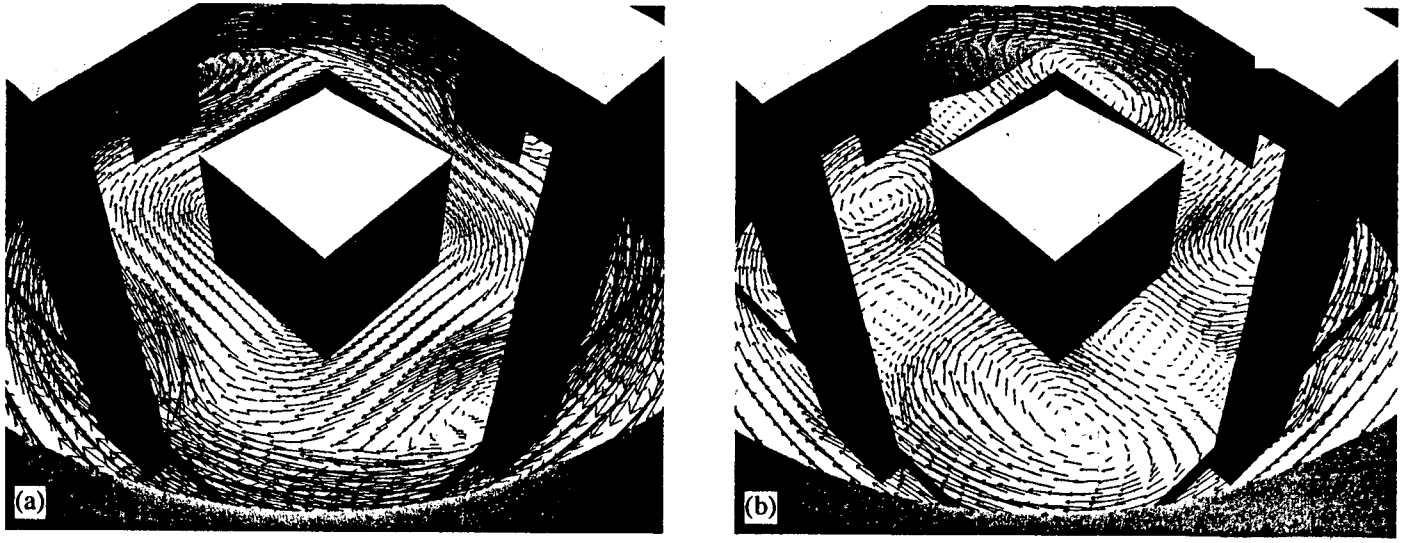

Figure 2. KDP results at two times (see Figure 1c), Reynolds number = 1267: (a) Velocity vectors after eight revolutions at constant rotation rate. (b) Velocity vectors after rotation is halted temporarily.

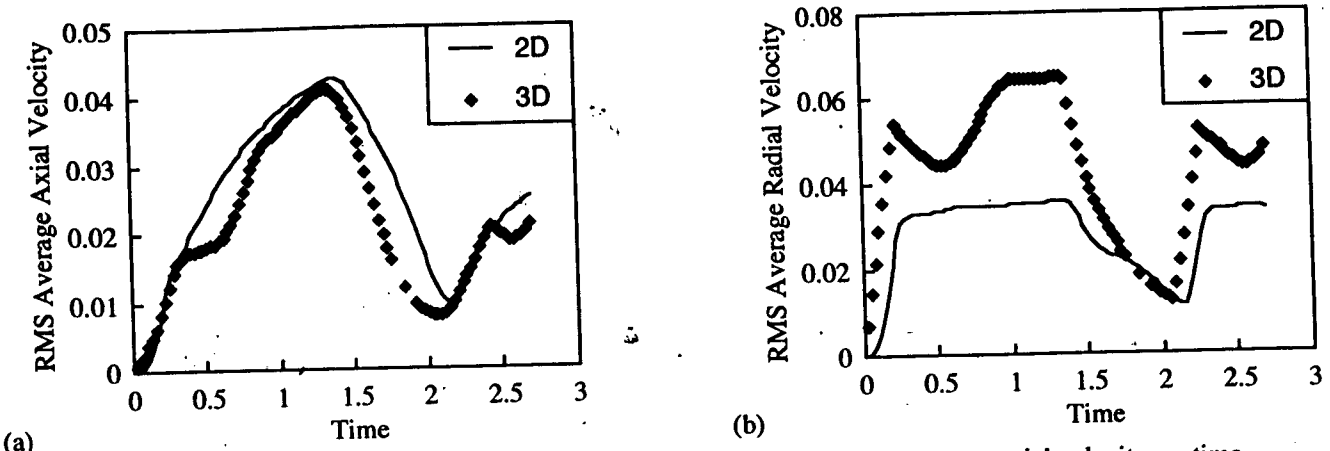

Figure 3. KDP results, Reynolds number = 1267: (a) Root-mean-square average axial velocity vs. time. (b) Root-mean-square average radial velocity vs. time. Rotation schedule shown in Figure 1c.

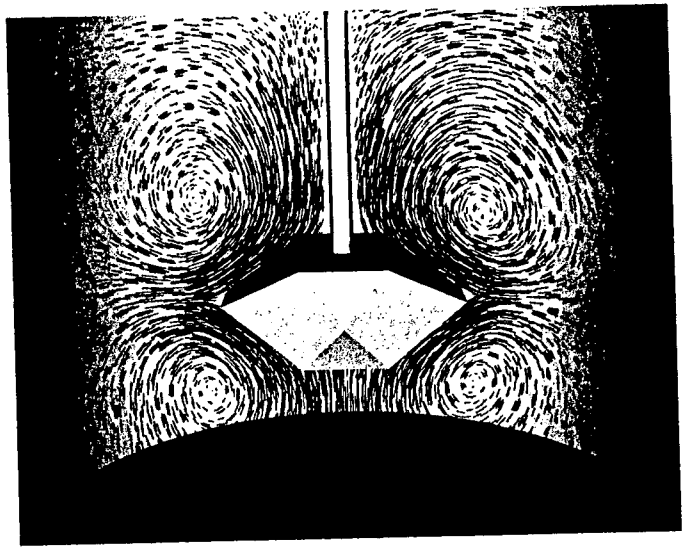

Figure 4. KTP results, steady-state, Reynolds number = 50.